Articles in PresS. J Neurophysiol (September 17, 2003). 10.1152/jn.00526.2003

# Heartbeat Control in Leeches: I. Constriction Pattern and Neural Modulation of Blood Pressure in Intact Animals

Angela Wenning, Gennady S. Cymbalyuk, and Ronald L. Calabrese*

Department of Biology, Emory University, Atlanta, GA 30322, USA

Running title: Heartbeat in Leeches

*Address for correspondence

Department of Biology, Emory University, 1510 Clifton Rd, Atlanta, GA 30322, USA

Phone (404) 727 0319; Fax (404) 727 2880;

## ABSTRACT

Two tubular hearts propel blood through the closed circulatory system of the medicinal leech. The hearts are myogenic, but are driven by a centrally generated motor pattern that controls heart rate and intersegmental coordination. In two consecutive papers, we address the question of how the motor pattern is translated into the pattern of diastole and systole of leech hearts.

We imaged the constriction patterns of the hearts in quiescent intact animals. In one heart, systole progresses rear-to-front (peristaltic coordination mode), while systole occurs nearly simultaneously in the other heart (synchronous coordination mode) with regular switches between these two coordination modes. Intersegmental phase relations between heart segments do not vary with changes in the heartbeat period. The peristaltic heart drives blood forward through itself and then rearward through the other longitudinal vessels. The synchronous heart does not seem to contribute to rearward flow along the body axis and may support segmental circulation instead.

Simultaneous monitoring of heart motor neuron discharge and the constriction of the corresponding heart segment in innervated, reduced preparations enabled us later to meld the constriction pattern with the fictive motor pattern described in the following paper (Wenning et al. 2003).

Current injections into one heart modulatory neuron while monitoring intravascular pressure from the corresponding heart showed that these neurons can acutely change diastolic and systolic pressure. However, they do not determine the

different systolic pressure profiles associated with the two coordination modes (Krahl and Zerbst-Boroffka 1983), which appear to result from the constriction pattern.

## INTRODUCTION

Stereotyped rhythmic movements, particularly those for continuous autonomous functions like breathing and neurogenic heartbeat (Calabrese and Feldman 1997), are attractive objects for study of how the nervous system programs movement. These movements are driven by central pattern generators that operate without the strong cycle-to-cycle sensory feedback observed in pattern generators for locomotor movements (Pearson and Ramirez 1997). Thus understanding the mechanisms for rhythmicity, timing, and phasing in these central pattern generators may provide greater insight into the control of movement than for other pattern generators.

Heartbeat in medicinal leeches is an ongoing motor pattern driven by a well-studied central pattern generator (Calabrese et al. 1995; Hill et al. 2002, 2003). The two lateral vessels along the body axis serve as hearts and are made of similar segmental 'modules' (Fig. 1) (Boroffka and Hamp 1969). Heartbeat in the leech is ongoing but not monotonous. Impedance measurements of the hearts in reduced preparations (Thompson and Stent 1976a) and intravascular pressure recordings in minimally dissected animals revealed two different coordination modes (Krahl and Zerbst-Boroffka 1983). At any given time, one heart produces a frontward peristaltic wave with high systolic pressure (50 mm Hg), while the contralateral heart produces nearly synchronous contractions with lower systolic pressures (20 mm Hg) (Fig. 1). Switches between these coordination modes are precipitous and reciprocal. Thus, the same heart performs different tasks and switches between them.

In this and the accompanying paper, we describe experiments aimed to understand to what extent heart performance, specifically the intersegmental coordination of the heart constrictions and the pressure profiles typical for the two coordination modes, is governed by the heartbeat central pattern generator. Leech hearts are myogenic but require phasic input for coordination and timing from the heart motor neurons (Maranto and Calabrese 1984b; Thompson and Stent 1976a). Additional input comes from the modulatory heart accessory neurons, which increase the beat tension of hearts in reduced preparations (Calabrese and Maranto 1984; Maranto and Calabrese 1984a,b). The leech heartbeat central pattern generator, a well-characterized network of 14 identified interneurons, determines the activity pattern of the heart motor and modulatory neurons (Calabrese et al. 1995; Hill et al. 2002, 2003).

In this first paper, we describe the constriction pattern of the two hearts in intact, restrained leeches using imaging techniques. We also describe the time relation between the onset of heart systole and the corresponding heart motor neuron burst using simultaneous recordings from the heart motor neurons and imaging of the hearts. Finally, we revisit the role of the heart modulatory neurons in shaping the different blood pressure profiles characteristic for the two coordination modes by simultaneous intravascular pressure recordings in the lateral hearts and intracellular recordings from a heart modulatory neuron in minimally dissected leeches. These experiments provide the necessary information for assessing the role of the fictive motor pattern, described in the accompanying paper (Wenning et al. 2003), in shaping the constriction patterns of the hearts in the intact animal.

Part of the results appeared in abstract form (Wenning and Calabrese 2002; Wenning et al. 2000).

## MATERIALS AND METHODS

Adult leeches (*Hirudo medicinalis* L.) were obtained from commercial suppliers (Leeches USA, Westbury, NY; Carolina Biological, Burlington, NC). Unfed juvenile leeches (2 – 4 months old) came from a colony in San Diego (courtesy of W. B. Kristan and K. A. French). Leeches were kept in artificial pond water at 16 °C. For all preparations, leeches were cold anaesthetized and pinned through both the anterior and posterior sucker in a stretched position. All dissections (described individually below) were completed within 60 min. Experiments were carried out at room temperature (20 – 22 °C).

### *Video imaging and analysis of heart constrictions*

Either juvenile leeches (40 – 100 mg) or small adult leeches (0.5 – 1 g) provided the intact preparations for video-imaging the heart constrictions and blood flow. Leeches were submerged in ice-cold artificial pond water. They were pinned through the anterior and the posterior sucker, ventral side up, in a stretched position (20 – 35 mm length for juveniles, 80 – 100 mm for adults) in a Sylgard®-lined dish. To improve imaging, juveniles were flattened by placing a cover slip over the whole animal. Adult leeches were flattened by pulling the lateral edges to the sides with small pins (one pair per segment).

Preparations were illuminated from below using fiberglass optics. Video clips (30 Hz) were taken with a CCD Camera in either color (DC 330) or black-and-white (Model 200T-RC or IR-1000) (Dage MTI Inc., Michigan City, Indiana, USA). Images were stored on a videocassette recorder.

A series of video clips were taken from each animal, capturing 3 – 6 neighboring segments at a time for 2 – 10 min (Fig. 3). Care was taken to have overlapping sets of segments to assess the intersegmental phase differences between the heart constrictions along the entire length of the leech body with respect to one reference segment. We used the Imaging Workbench software (v. 4.0; Axon Instruments Inc., Foster City, CA) for an automated analysis of heart diastole and systole. Light intensity ($I$) transmitted through the preparation in user defined analysis windows drawn around corresponding sections of the lateral heart tube in each segment visible in a movie clip (see image at 1190 ms of Fig. 3) was digitized and collected. The rhythmic filling and emptying of the heart with red blood caused oscillatory changes in the intensity of the transmitted light in the analysis windows (Fig. 3, bottom trace) and these "optical signals" were used in our analysis of heartbeat. The absolute values of the digitized signals depended on the size of the analysis windows and the visibility of the heart tube in a given segment and were therefore not comparable between different preparations or even between different heart segments of the same preparation.

Data series of these optical signals were imported into Kaleidagraph (Synergy software, Reading, PA) for plotting and into Matlab (Mathworks, Natick, MA) for data analysis. First, we identified the part of the waveform representing

emptying of the heart, i.e. systole, by comparing the optical signals with simultaneously acquired frame-by-frame measurements of the changes in heart tube diameter (Fig. 4). Next, we defined the start of systole (constriction) of the heart, as the phase marker. In the optical data series, the start of systole was estimated best by the moment in time halfway between maximum filling of the heart segment (trough of the optical signal, Fig. 4, maximal diastole), and the moment in time of the maximal growth of the optical signal corresponding to emptying, i.e. where the first derivative ($\frac{dI}{dt}$) of the intensity trace was a maximum ($\frac{d^2I}{dt^2} = 0$) (Fig. 4). The analysis program written in Matlab was then used to calculate the cycle period of the heartbeat and the intersegmental phase difference between a given heart segment and a reference heart segment. The cycle period of segment *i* was defined as the interval ($T_i$) between occurrences of the phase markers (i.e. attainment of systole) in two consecutive heartbeat cycles of the optical signal obtained from segment *i*. The phase ($\phi_{i\text{-}j}$) of a given heart segment *j* was determined on a cycle-by-cycle basis using segment *j* as a reference ($\phi_{i\text{-}j} = -\phi_{j\text{-}i}$). The phase of heart segment *i* was defined as the difference between the time of occurrence of the phase marker of segment *i* ($t_i$) and the time of occurrence of the phase marker of the reference segment *j* ($t_j$) in the same cycle divided by the reference cycle period ($T_j$). Phase is expressed in % by $\phi_{i-j} = \left( \frac{t_i - t_j}{T_j} \right) \times 100$. A phase of 0% indicates that a segment is in phase with the reference segment, while a phase of 50% indicates an antiphasic or out-of-phase relationship. A positive phase difference indicates that the constriction of the

reference segment leads, while a negative phase difference indicates it lags the constriction of a given heart segment.

All intersegmental phase differences were referenced to the heart segment 10 in a multi-step process. First, a 'local' reference heart segment was chosen in each individual video clip, for example, segment 8 in a video clip of segments 5, 6, 7, and 8. The next video clip of segments 8, 9, 10, and 11 allowed us to establish the phase difference between the hearts in segment 8 and segment 10, thereby concatenating the data obtained from the two video clips. Side-to-side phase differences were determined for the local reference heart segment within each video clip.

*Simultaneous extracellular recordings from the heart motor neuron and imaging of the heart constrictions*

Innervated, reduced preparations were used to record *en passant* from a heart nerve while imaging the constriction pattern of the corresponding lateral heart segment. Leeches were opened dorsally and covered with leech saline ([mM]: 115 NaCl, 4 KCl, 1.8 $CaCl_2$, 10 Glucose, 10 HEPES buffer and adjusted to pH 7.4 with NaOH or HCl). In such preparations, the dorsal vessel (a major collecting vessel) and much of the capillary beds are cut and blood flow is compromised. To expose the lateral heart in two segments, the crop wall and the dorsoventral muscles were removed, and the dorsal branch of the posterior nerve root was cut in these segments. The rest of the peripheral innervation was left intact. The animal was superfused with leech saline for the duration of the experiment at 3 – 4 ml/min. Bath volume was about 30 ml.

Of the three nerves supplying the lateral heart, the Y nerve (Wenning et al. 2003) requires the least damaging preparation and was therefore used for *en passant* recordings. For extracellular recordings, the Y nerve was isolated from its accompanying dorsoventral muscle fibers, and its distal part was aspirated in a small loop into a suction electrode made of a tapered glass capillary (o.d. 1 mm) filled with leech saline. The protocol for extracellular recordings is described in detail in Wenning et al. (2003). To determine the coordination mode of the heart while imaging, two Y nerves were recorded simultaneously, which enabled us to assess the intersegmental phase difference between the heart motor neurons. Video clips (30 Hz) were taken with a CCD Camera (Model DC 330) trained in succession to the corresponding heart sections of each of the same two segments used for electrophysiological recordings.

To synchronize the acquisition of electrophysiological data with image data we employed two different methods. In the first method, we used pClamp protocols (Axon Instruments) to trigger data acquisition by the Axon Imaging Workbench software. However, due to the long transfer time that the program needed to clear the memory buffer, data acquisition at full video rate was limited to 30 s. We used the second method to obtain longer recordings. We triggered a short (50 ms) light pulse, and simultaneously acquired the trigger signal with the electrophysiological data and the light pulse with the video camera and cassette recorder for later synchronizing. Image data were later digitized using Imaging Workbench software. To assess the constriction pattern relative to the bursts of action potentials of the corresponding heart motor neuron, the heart diameter in a given segment was

measured frame-by- frame directly from the video screen. During a burst of action potentials (i.e. the burst phase), a measurement was taken from every 10th frame (interval 330 ms) and between bursts of action potentials from every 20th frame (interval 660 ms). For each experiment, 2 – 4 heartbeats per coordination mode were analyzed. For comparison among preparations, the heart diameter was normalized by the first five measurements following the first spike of the heart motor neuron burst. This average corresponded to the end-diastolic diameter in the first heartbeat cycle of a given preparation and was set to 100%.

The intersegmental phase differences between the heart motor neuron bursts and the instantaneous spike frequencies were calculated using a spike train analysis program written in Matlab. The analysis is described in detail in the accompanying paper (Wenning et al. 2003).

*Simultaneous extracellular recordings from the vascular nerves and the heart modulatory neurons*

Denervated nerve cords were used to record the activity from heart modulatory neurons in the peripheral nerves. The preparation and the recording techniques are described in the following paper (Wenning et al. 2003). In brief, leeches were opened dorsally and the vascular nerves as well as the Y nerve were exposed in 4 – 6 segments. All other peripheral nerves were cut. The head and tail brains were left attached to the ganglion chain and the preparation was superfused with leech saline at 3 – 4 ml/min.

To determine the extent of innervation of the hearts by the heart modulatory

neurons that are present in segments 5 and 6, we used paired extracellular recordings from one heart modulatory neuron cell body and a heart nerve. To expose the soma of a heart modulatory neuron, the segmental ganglion was freed from the surrounding ventral vessel, the segmental nerve roots cut, and the ganglion flipped to gain access to the ventral surface. The anterior lateral packet was desheathed and a suction electrode placed near the putative heart modulatory neuron soma. Gentle suction brought the cell body inside the electrode. The heart modulatory neuron was identified by size, location and its activity pattern. Positive identification of a peripheral spike of the heart modulatory neuron required the occurrence of a spike at a fixed delay in one of the heart nerves in different segments. The fixed delay was determined through the analysis of averaged electrical activity in a time window triggered by the spikes in the soma. Total recording time was between 60 – 120 min.

*Simultaneous recordings of intravascular pressure and heart modulatory neuron activity*

Minimally dissected preparations were used to record intravascular pressure and heart modulatory neuron activity simultaneously. To minimize longitudinal movements, adult leeches were pinned in a stretched position (dorsal side up) in artificial pond water for a period of 30 – 120 min, after which they were stretched maximally. Prior to dissection, the artificial pond water was replaced with leech saline, and the animal was repositioned (ventral side up).

To expose the heart in segment 8 on the right body side, a lateral incision was made from segment 7 (last annulus) to segment 9 (middle annulus). Integument and

muscle layers were forced and held apart with small hooks. Care was taken to leave the protective connective tissue around the lateral heart and the dorsoventral muscles intact.

To gain access to the appropriate heart accessory neuron in segment 6, a second incision was made from segment 5 (last annulus) to segment 6 (last annulus) on the ventral midline. Integument and muscle layers were forced and held apart with small hooks. The bulging mass of sex organs was kept in place by 4 – 6 smaller hooks. An incision in the ventral vessel exposed the segmental ganglion. A platform (flattened and blackened insect pin) was slipped under the ganglion and secured with dental wax at the side of the dissection dish.

Intravascular pressure was monitored using a glass capillary (o.d. 1.5 mm) with a tip of 50 – 70 μm o.d. inserted into the lateral heart (Fig. 2). The recording pipette was connected to a precalibrated, disposable pressure transducer (DPT, Ohmeda; courtesy of Becton & Dickinson, Ventura, CA) fixed at the height of the recording site. To maximize the pressure signal, all connections between the recording site and the transducer were rigid. The transducer had a volume displacement of less than $1x10^{-10}$ l per mm Hg. From a reservoir, the entire system was filled with leech saline that had been filtered (Nalgene PES 0.45 μm) and degassed (using negative pressure for 2 h). To visualize developing air bubbles, the saline was colored prior to filtering with Fast Green (Sigma Chemicals, St. Louis, MO). A three-way stopcock allowed (1) connecting the transducer to the reservoir (for filling the system) (2) venting the transducer to air (for zeroing) and (3) connecting the transducer to the recording probe (Fig. 2). After the recording pipette

had been filled to the tip, the reservoir was shut off. When the recording pipette was submerged into saline and on the level of the recording site (i.e. the leech heart), the transducer was briefly vented to air ('zeroed'). Using a micromanipulator, the recording pipette was inserted into the lateral heart at a flat angle with its tip facing the rear. In successful recordings, regular pressure pulses were recorded for about 60 min. Pressure signals were amplified (Model 410 Instrumentation Amplifier, Brownlee Precision Co., Santa Clara, CA). Data were acquired at 2.5 kHz and were low-pass filtered at 80 Hz for display purposes.

After establishing a satisfactory pressure reading, the corresponding heart modulatory neuron was impaled. Heart modulatory neurons were identified based on their position, soma size and their characteristic pattern of activity (Calabrese and Maranto 1984). Intracellular signals were monitored with the Axoclamp 2A (Axon Instruments). Microelectrodes were filled with a mixture of 4 M potassium acetate and 20 mM KCl and had resistances of 20 – 25 MΩ. Recording and current injection (bridge) techniques were conventional. In successful recordings, the heart modulatory neuron was held for about 30 min.

*Statistics and nomenclature*

Values are expressed as means of the averages of individual experiments ± SD. A student's t-test (paired or unpaired, see text) assessed statistical significance.

Segments are numbered according to Kristan et al. (1974). Segment #1 is assigned to the metameric body segment innervated by the most anterior (non-

cephalic) ganglion of the ventral nerve cord. The remaining segments and ganglia are numbered consecutively up to #21, which is just anterior to the tail brain.

## RESULTS

To monitor the pattern of diastole and systole along the hearts of intact, restrained animals, we devised a non-invasive imaging technique and appropriate analysis software. The weak pigmentation of juvenile leeches provided good contrast for the flow of red blood, while adult leeches, which are not as translucent, gave weaker signals.

The image series of Fig. 3 shows midbody segments 8 to 10 in an intact juvenile leech (see also the movie). In the first image (0 ms), the right hearts of segments 8 and 9 (bottom) are filled with blood, followed by filling of the heart in segment 10 (170 ms). Emptying also occurs from front to back, starting with segment 8 (340 ms) followed by the hearts in segment 9 (510 ms) and 10 (680 ms). In the contralateral left heart (top), filling starts from the rear with segment 10 (510 ms) followed by segments 9 (680 ms) and 8 (850 ms), when all visible left heart segments are filled. The heart in segment 10 empties first (1020 ms), followed by segment 9 (1190 ms). The different sequential orders in which the two hearts undergo diastole and systole illustrate the two coordination modes of leech hearts: the left heart with rear-to-front flow is in the peristaltic coordination mode while the right heart with seemingly front-to-rear flow is in the synchronous coordination mode (Thompson and Stent 1976a). The image series also shows that the hearts in

these midbody segments beat in antiphase: while one side is in diastole and fills, the other side is in systole and empties.

For an automated analysis of the progression of systole along the hearts, analysis windows, shown in the last image (1190 ms; Fig. 3), were placed around corresponding heart sections. Rhythmic emptying and filling of the hearts caused rhythmic light intensity changes. This oscillatory optical signal was digitized and correlated with simultaneous diameter measurements of the hearts. The trough of the optical signal (maximal light absorption) corresponded to the maximal diastole (Fig. 4; shaded circles) and the fast decrease of light absorption after filling of the heart corresponded to emptying (systole), which coincided with the decrease in heart diameter, i.e. constriction. We determined the intersegmental phase differences between all segments for both hearts along the entire length of the animal. We chose a phase marker equivalent to the attainment of systole (shaded diamond; Fig. 4), and used it to calculate the cycle period and the phase differences between heart segments (see methods for details). The exact alignment varied somewhat because it depended upon the identification of the point of end-diastolic filling, i.e. the trough of the optical signal, which was variable.

*Intersegmental coordination of systole in the peristaltic and synchronous coordination modes*

We calculated the intersegmental phase differences for the attainment of systole (referred to as 'systole' hereafter) for heart segments 3 to 18 in 17 intact leeches (8 juveniles, 9 adults). The average heartbeat period was 4.7 ± 0.7 s in the

juvenile leeches, ranging from 2.9 to 6.9 s, and 10.0 ± 3.5 s in the adults, ranging from 5.8 to 15.1 s.

Figure 5 shows the regular oscillatory optical signals associated with each heartbeat for midbody segments 8 to 10 on both sides in an intact juvenile leech. The optical signals are from the same preparation as used for the image series (Fig. 3), and the shaded area in the expanded optical signals on the left corresponds to the video frames shown in Fig. 3. Phase differences are referenced to the heart in segment 10, which is assigned 0%. A positive phase difference indicates that the constriction of the reference segment leads, while a negative phase difference indicates it lags the constriction of a given heart segment.

On average, the systole in segment 9 (L,9) in the left heart, which was in the peristaltic coordination mode, lagged by 7 ± 3% with respect to reference segment 10 (L,10), and the systole in segment 8 (L,8) lagged by 16 ± 4% (Fig. 5; top panel, left). Systole of segment 9 (R,9) in the right heart, which was in the synchronous coordination mode, was in phase with segment 10 (phase difference +1 ± 4%), while segment 8 (R,8) led by 7 ± 2%, i.e. constricted earlier. The heart in segment 10 attained systole first on the peristaltic side (solid vertical line in the expanded optical signals (left)) and could thus contribute to the filling of the hearts in segments 9 and 8, which were still in diastole. Conversely, in the synchronous coordination mode, heart segment 8 constricted first and could thus deliver blood into heart segments 9 and 10, which had not entered systole yet. Front-to-rear flow appeared to be restricted, however, because the time available for filling was short due to the small phase differences on the synchronous side.

Switching between coordination modes was always reciprocal (Fig. 5; movie). Switch period and the number of beats between switches varied little in a given preparation but were quite variable across preparations (Table 1).

In contrast to the regular constriction pattern seen in midbody segments, the pattern in the front and rear segments is more complicated and more variable (Fig. 6). In anterior segments 3 and 4, the hearts spend more time in full diastole, and systole is brief when compared to segments 5 and 6, which stay constricted longer (Fig. 6, left). On the synchronous side, systole occurs almost simultaneously in segments 3 to 6. In the front and middle segments, phase differences between successive segments progress smoothly but are more erratic in the rear (Fig. 6, right). For example, heart segment 18 constricts later than heart segment 16, even in the peristaltic coordination mode. For comparison, we imaged adult leeches and found that blood flow was always regular in the anterior segments but often irregular from segment 12 rearwards. Sometimes we observed apparent arrests of heartbeat lasting for several cycles.

In the posterior heart, the segmental phase differences between the front and rearmost segment in a particular video clip were sometimes similar in both coordination modes. Assignment of the coordination mode was therefore also based on the side-by-side phase differences (see paragraph below). While beating roughly out of phase in the middle segments, there was a distinct phase lead of about 15 to 20% for the synchronous side in segment 15.

Across preparations, intersegmental phase differences did not vary with period. Juvenile leeches had shorter heartbeat periods than adults, yet phase

relations were similar (Fig. 7*A*). To further emphasize this similarity between juvenile and adult leeches, we plotted their unilateral average intersegmental phase differences separately (Fig. 7*B*). The phase diagram shows the systole and the diastole in each heart segment, referenced to the systole in the heart of segment 10. There was a smooth rear-to-front progression of systole in the peristaltic coordination mode. In both juveniles and adults intersegmental phase difference between segments 14 and 4 traversed 55% (5.5% per segment), while rear segments 15 to 17 constricted nearly simultaneously. There was a front-to-rear progression of systole in the synchronous heart between segments 3 and 13 traversing about 20% of phase (2% per segment). Phase progression was smoother in the juveniles than in the adults where phase differences were generally more variable. In the rear, phase relations were more variable in both juvenile and adult leeches.

*Side-to-side coordination of systole in intact leeches*

To understand blood flow in the intact leech, we need to know the coordination between the two hearts. The bilateral phase diagrams of Fig. 8 summarize the side-to-side phase differences for juveniles (left) and adults (right). Systole in the heart of segment 10 on the peristaltic side is assigned 0% phase (dotted line). The phase difference between the peristaltic and the synchronous heart in segment 10 was similar in juvenile and adult leeches (+60.2 ± 11.4%; 8 juveniles; +62.1 ± 5.1%; 9 adults), and the systole in the heart segment 10 on the synchronous side was shifted accordingly to the right. To illustrate the coordination in the rear segments, the peristaltic side is duplicated and shifted to the right by 100% (dotted

line).

The hearts in segment 9 constricted in antiphase. In the front, heart constrictions came nearly in phase, with the peristaltic side leading the synchronous side by about 15%. In the rear, heart constrictions also came nearly in phase up to segment 15, with the synchronous side leading by about 15 to 20%. Rear segments 16 to 18 constricted almost simultaneously (Fig. 8).

The rear-to-front progression of systole in the peristaltic coordination mode supports rear-to-front blood flow and is in accordance with previous findings that, in addition to blood entering from the two afferent vessels, blood also enters from posterior segments (Krahl and Zerbst-Boroffka 1983) (Fig. 1). Blood flow had been thought to be rear-to-front in the hearts for both coordination modes (Boroffka and Hamp 1969) but the slight front-to-rear progression of systole in the synchronous coordination mode shown here and the visual observations of blood flow in our video clips do not support forward blood flow (Figs. 3, 6, and 7).

*Correlation of heart motor neuron activity and heart constrictions*

Leech hearts are innervated by 16 pairs of segmentally arranged motor neurons (Thompson and Stent 1976a) which form neuromuscular junctions on the heart muscle cells (Maranto and Calabrese 1984a). As shown by intracellular recordings from both the heart muscle and its innervating motor neuron, excitatory junctional potentials from the heart motor neurons summate in the heart muscle cells and give rise to plateau-like potentials (Maranto and Calabrese 1984b). The heart

motor neurons reset and entrain the heart's intrinsic electrical and contractile myogenic rhythms (Maranto and Calabrese 1984b).

We wanted to align the systole in a specific heart segment with the electrical activity of the corresponding heart motor neuron to later combine the constriction pattern described here with the fictive motor pattern described in the following paper (Wenning et al. 2003). We therefore monitored heart motor neuron discharge and the constriction of the corresponding heart segment using simultaneous video monitoring and *en passant* recordings and determined the phase difference between heart constriction and heart motor neuron activity (Fig. 9, cartoon, and Methods). To visualize the hearts and have access to the heart nerves, we used reduced preparations in which the innervation was left intact but circulation was disrupted and focused on segments 4, 7, 10, and 14.

We chose the Y nerve for *en passant* recording of the heart motor neuron discharge because it requires the least dissection (see Wenning et al. (2003) for a description of the heart innervation). In these preparations, the automated analysis of heart constriction described above for intact leeches did not yield reliable optical signals. Instead, we measured the heart diameter frame-by-frame. For each preparation, we referenced the diameter changes of the heart tube to the end-diastolic diameter of its first cycle and set this value to 100%. On average, the lateral hearts constricted to between 70 and 40% of their end-diastolic diameter. Here, systole was defined as a drop by 20% of the full constriction in that heart segment and corresponded well to the systole defined in the analysis of the optical signals in intact animals (Fig. 4). We referenced the systole to the median spike of the

corresponding heart motor neuron burst (see Wenning et al. (2003) for a detailed description of the extracellular recordings from the heart motor neurons).

The example shown for segment 14 illustrates the timing of heart constriction with respect to the median spike in the corresponding heart motor neuron during a switch in coordination mode (Fig. 9). Constrictions are of the same magnitude in both coordination modes, albeit shorter during the switch. Figure 10 shows that timing of heart systole with respect to motor neuron discharge was not uniform along the body axis. In the more anterior segments 4 and 7, the hearts constricted around the median spike of the corresponding motor neuron burst and the constriction outlasted the heart motor neuron burst. In the more posterior segments 10 and 14 (Figs. 9 and 10) as well as 17 and 18 (data not shown) heart constrictions started before the median spike and hearts dilated while the heart motor neuron was still active. Furthermore, constrictions in the front segments started at higher frequencies of the heart motor neuron discharge than constrictions in the rear. The timing of, and the change in, heart diameter were segment-specific regardless of coordination mode. The heart diameter changed most in the rear segments, to about 40% of its end-diastolic diameter (Fig. 10). We conclude from these experiments that the hearts constrict in a fixed phase relation with respect to their corresponding heart motor neuron bursts.

*Action of the heart modulatory neurons on blood pressure*

Two pairs of heart modulatory neurons, present in segmental ganglia 5 and 6, innervate the contralateral heart sections of segments 5 and anterior, and segments 6

and posterior, respectively (Calabrese and Maranto 1984; Maranto and Calabrese 1984b). We used paired extracellular recordings from the heart nerves and the corresponding heart modulatory neuron to re-examine their contribution to heart innervation with special attention to posterior segments in denervated nerve cords (Fig. 11*A*). Action potentials from the heart modulatory neuron in segment 6 were recorded with a fixed delay in the heart nerves up to segment 12 (Fig. 11*B*) but not in segments 13 (N=2), 14 (N=2) and 16 (N=1). Action potentials recorded in the soma of heart modulatory neurons in segment 5 were also recorded in the heart nerves of segments 5, 4 (data not shown) and 3 (Fig. 11*C*), confirming earlier results (Calabrese and Maranto 1984). Thus, the heart modulatory neuron in segment 6 extends into the heart nerves up to segment 12, while the heart modulatory neuron in segment 5 extends into the heart nerves of segments 3, 4, and 5.

Occasionally, extracellularly recorded action potentials were larger than those of the heart motor neurons and could be reliably identified on an outgoing nerve (Fig. 11*D*, top trace, asterisks). We use this example to show the different bursting patterns of the heart modulatory neurons in segment 5 and 6 in both coordination modes in denervated nerve cords. In the heart modulatory neuron of segment 5, action potentials were not grouped in clear bursts (Fig. 11*D*, top trace, asterisks). On average, the heart modulatory neurons in segment 5 have an irregular, rather tonic firing pattern. The heart modulatory neurons of segment 6 had regular bursts and mean spike frequencies were on average lower (0.69±0.46 Hz) in the synchronous coordination mode than in the peristaltic coordination mode (0.85±0.40 Hz; means of 7 preparations; $p < 0.02$; paired t-test).

The paired recordings from heart motor and modulatory neurons enabled us to calculate the phase relations between the co-projecting heart motor neurons and the heart modulatory neuron in segment 6. The heart modulatory and motor neurons burst roughly in phase on the peristaltic side, while the burst of the heart modulatory neuron of segment 6 is out of phase with the co-projecting heart motor neurons on the synchronous side, confirming earlier results (Calabrese and Maranto 1984). The pattern of activity of the heart modulatory neurons differed in extracellular (Fig. 11*D*) *vs.* intracellular recordings (Fig. 12*C* and *D*; Calabrese and Maranto 1984). Lower frequencies of discharge and less well-defined bursts were observed in extracellular recordings, especially in the heart modulatory neuron 5 (Fig. 11*D*).

The heart modulatory neurons form synapses on the heart muscle cells (Maranto and Calabrese 1984a), induce myogenic activity in quiescent hearts, and accelerate the rhythm of hearts that are already myogenic. The heart modulatory neurons can also increase the beat tension in hearts that are entrained by rhythmic discharge of the heart motor neurons driven by the heartbeat central pattern generator (Calabrese and Maranto 1984). Because the hearts display different pressure profiles in the two coordination modes (Krahl and Zerbst-Boroffka 1983) and because the heart modulatory neurons modulate the contractile strength of the hearts (Calabrese and Maranto 1984), we examined whether blood pressure is determined by the heart modulatory neurons (Fig. 12). We monitored intravascular pressure in the lateral heart of segment 8 in minimally dissected leeches, while recording intracellularly from the contralateral heart modulatory neuron in segment 6 (Fig. 12, cartoon). Systolic pressures are about twice as high in the peristaltic

coordination mode as in the synchronous coordination mode (Fig. 12*A*). Systolic pressure was between 20 – 45 mm Hg in the peristaltic coordination mode and 10 – 20 mm Hg in the synchronous coordination mode. To record intracellularly from the heart modulatory neuron in the segmental ganglion we had to open the ventral vessel. The inevitable blood loss might be responsible for somewhat lower systolic pressures than reported previously (peristaltic side: 48 ± 14 mm Hg; synchronous side: 26 ± 11 mm Hg; Krahl and Zerbst-Boroffka 1983).

Depolarization of the heart modulatory neuron in segment 6 (+1 nA, 30 – 50 s) led to an increase of the systolic pressure both in the peristaltic coordination mode (from 21 to 36 mm Hg; data not shown) and, more pronounced, in the synchronous coordination mode (from 11 to 30 mm Hg) as well as to an increase of the diastolic pressure (Fig. 12*B*). Conversely, hyperpolarization of the heart modulatory neuron (-1 nA, 30 – 50 s) resulted in a decrease of the systolic pressure in the peristaltic coordination mode (Fig. 12*C*, first current injection) and across a switch from the peristaltic to the synchronous coordination mode (Fig. 12*C*, second current injection). It took 1 – 2 cycles for the systolic pressure to change upon injecting current into the heart modulatory neuron and sometimes more cycles to wane. This delayed onset and waning of the peripheral effects of the heart modulatory neuron is consistent with its modulatory role (Calabrese and Maranto 1984). Neither the heartbeat period nor the timing of the switching was affected by the depolarization or hyperpolarization of the heart modulatory neurons. We conclude from these experiments that the heart modulatory neurons may modulate, but do not determine, the difference in systolic blood pressure in the two hearts.

## Discussion

Two longitudinal vessels serve as hearts in the leech (Boroffka and Hamp 1969). Aided by sphincters and valves (Fig. 1; Hammersen et al. 1976), they propel blood along the body axis and distribute blood into the segmental circulation. Leech hearts are myogenic but heart rate and the coordination of the constriction of the individual heart segments are shaped by the motor pattern, which in turn is driven by the heartbeat central pattern generator (Calabrese and Maranto 1984; Calabrese et al. 1995; Hill et al. 2003; Thompson and Stent 1976a,b). Leech hearts switch between two coordination modes termed the peristaltic coordination mode and the synchronous coordination mode, associated with different systolic pressure profiles (Krahl and Zerbst-Boroffka 1983; Thompson and Stent 1976a). Our segment-by-segment analysis of the coordination of systole shows that in the peristaltic coordination mode posterior heart segments fill and empty first, and that in the synchronous coordination anterior heart segments fill and empty first (Fig. 3). Intersegmental phase differences do not vary with the heartbeat period (Fig. 7*A*), perhaps ensuring similar hemodynamics when the heart rate changes.

### *Interaction of neuronal activity and heart performance*

Heart systole in the intact animal results from the interaction of the muscular heart tubes with both the heart modulatory and motor neurons, and also with the variable load associated with blood entering and leaving the hearts. Timing of the constriction in the intact leech might additionally depend on other factors including

afferent feedback, neuromuscular transform, the variable load environment, and the hydrodynamics of the vascular system.

Heart modulatory neurons increase the beat tension in hearts that are entrained by the heart motor neurons through the central pattern generator (Calabrese and Maranto 1984), suggesting a role in shaping the different systolic pressure profiles associated with the two coordination modes. As shown here, identified heart modulatory neurons do not project to heart segments more posterior than segment 12 but systolic pressures still differ as far back as segment 14 (Krahl and Zerbst-Boroffka 1983). The heart modulatory neurons may modulate blood pressure when their pattern of activity changes (Fig. 12*B* and *C*). However, they do not determine the different systolic pressure profiles characteristic for the two coordination modes. Rather, these strikingly different systolic pressures seem to be generated by the intersegmental coordination of systole, and hence by the rhythmic activity pattern of the heart motor neurons (see below).

Each heart motor neuron burst caused a constriction in the corresponding heart segment but with segment-specific phase differences both with respect to onset and waning of the systole (Figs. 9 and 10). In principle, these differences may be due to differences in motor neuron discharge (spike frequency, duty cycle) at the neuromuscular junction, of the contractile properties of the heart muscle cells, and/or of the hemodynamic load and vessel mechanics in intact *vs.* reduced preparations. For example, in intact animals, filling of the hearts dilates the heart tube, which might delay its constriction. Conversely, because there are no antagonistic muscles, rapid distension in leech hearts may rely on incoming blood. Expansion of the hearts

during diastolic filling is limited by the elasticity of the heart and potentially by hydroskeletal constraints. To resolve this issue we need to study the neural control of the coordination of the hearts and the contractile incoming vessels and heart performance in minimally dissected animals.

Switching between coordination modes is under neural control (Calabrese 1977). Whether considering the fictive motor pattern (Calabrese and Peterson 1983; Lu et al. 1999; Thompson and Stent 1976a; Wenning et al. 2003), the motor pattern in minimally dissected leeches (Krahl and Zerbst-Boroffka 1983) or intact leeches (this study), switching between the two coordination modes is always reciprocal. Switch period and the number of beats between switches vary little in a given preparation but are quite variable across preparations (Table 2).

*Circulation*

The segment-by-segment analysis of the pattern of systole in the peristaltic and the synchronous hearts results in an improved understanding of circulation in the leech. Most importantly, we found that blood flow is not always forward in the hearts as previously thought (Boroffka and Hamp 1969).

Sphincters and valves are present in the contractile vessels and aid in directing blood flow. The hearts have a main sphincter in the posterior part of each segment (Fig. 1). The main sphincter appears as a thickening of the heart musculature wall (Maranto and Calabrese 1984a) and obstructs blood flow early in systole. The initial portion of the single segmental outlet, the lateroabdominal vessel, is muscular and may be closed off during systole (Hildebrandt, 1988). The

orifices of the two afferent vessels bear multiple pine cone-shaped fibrous villi, which surround the opening (Hammersen et al. 1976). Non-muscular in nature, they operate as (passive) valves (Fig. 1). When systolic pressure in the heart overcomes the pressure in the afferent vessels, the villi are pushed back into the orifice preventing backflow (Fig. 1, emptying in systole).

In the peristaltic coordination mode, nearly simultaneous contractions in segments 17 to 14 act as a resistance to backflow that is followed by a peristaltic contraction wave propelling the blood forward (Figs. 7 and 8). Filling of the hearts in segment 13 and anterior is through the two afferent vessels and from the rear (Fig. 1). The lateroabdominal sphincter is open for the initial phase of the contraction cycle in each segment and therefore some blood may enter the segmental circulation (Hildebrandt 1988). The valves to the afferent vessels close early in systole, preventing flow back into the periphery. At the same time, the sphincters located in the posterior portion of the hearts close and prevent backflow during the rear-to-front peristaltic wave. The peristaltic heart pumps blood into the vessels of the front sucker region perfusing the associated capillary beds and causing rearward flow into the dorsal and ventral vessels and the synchronous heart. We hypothesize that the peristaltic heart is the main propulsive force to drive blood along the body axis to the front as well as back to the rear.

Rearward blood flow into the synchronous heart through interconnecting vessels in the front sucker region is limited because systole begins soon after the end of the peristaltic wave in the opposite heart (Fig. 8). The synchronous heart, however, does not contribute to flow into the anterior capillary beds or into the

dorsal and ventral vessels as had been thought previously (Boroffka and Hamp 1969). Rather, as suggested by Hildebrandt (1988), the synchronous heart may support segmental circulation through the lateroabdominal vessels in each segment (Hildebrandt 1988). However, our results do not support propulsive rearward flow. Systole progresses front-to-rear but phase differences from segment to segment are much smaller than on the peristaltic side (Fig. 7), and it is difficult to envision how such a small contraction progression can support propulsive rearward blood flow. Moreover, near synchrony in segmental contraction should support peripheral flow by restricting both forward and rearward flow; the main sphincters along the synchronous heart close in rapid succession, the valves to the afferent vessels close, and blood, trapped in one heart segment, may be forced out mainly through the lateroabdominal vessel into the peripheral circulation (Fig. 1). The absence of a distinct pressure prepulse, which would signal a propulsive force from an anterior segment, and the lower systolic pressures in the synchronous heart (Figs. 1 and 12*D*) would seem to support this view. However, we cannot predict at this point how much of the blood entering a given segment in the synchronous heart ends up in the peripheral circulation of that segment or flows into more posterior segments. Neither video imaging as used in this study nor the two-point pressure recordings from various locations employed previously (Hildebrandt 1988; Krahl and Zerbst-Boroffka 1983) are suitable to track a defined bolus of blood.

In segmented animals with a closed circulatory system like annelids, circulation serves serial and parallel vascular beds at the same time. The demands on circulation – rapid blood transfer to deliver nutrients and oxygen along the body

axis and slower circulation along the segmental capillary beds – are met differently among annelids. The design, albeit not the evolutionary origin, of the annelid vasculature is deceptively similar, yet, the physiological role of these vessels differs, and especially which vessel(s) play the role of the heart(s). For example, in the giant earthworm *Megascolides* with up to 1000 segments, the dorsal vessel and its connections to the ventral vessel serve as hearts. Using tracers to follow blood distribution revealed that circulation differs in the front, middle and rear of the animal, effectively dividing the animal into different circulation zones along the body axis. Jones et al. (1994) suggested that the rapid circulation seen in the anterior 15 to 20 segments delivers oxygenated blood to the cephalic structures and the reproductive system, while the much slower circulation along the rest of the worm (segments 40 and posterior) serves largely vegetative functions. Circulation in the leech is also compartmentalized. Here, the two longitudinal vessels serving as hearts are coordinated differently and switch roles, effectively dividing the animal into two bilateral circulation zones. The resulting complex flow pattern is yet a different solution for an animal with a highly segmented body plan, but with many fewer segments, to create a powerful peristaltic pump to rapidly move oxygen from the skin and nutrients from the capillary beds of the intestine to the front. At the same time, the other heart forces blood though the dense parallel capillary beds of segmental circulation.

The scheme of circulation presented here for the leech implies that the constriction patterns of the individual heart segments along the body axis determine systolic pressures. Larger intersegmental phase differences and a rear-to-front wave

of constrictions in the peristaltic coordination mode lead to higher end-diastolic filling and hence higher systolic pressure. Smaller intersegmental phase differences and almost synchronous constrictions in the synchronous coordination mode lead to filling only from the side vessels and hence lower systolic pressure. In the accompanying paper (Wenning et al. 2003), we will explore whether the fictive motor pattern defined in denervated nerve cords matches the constriction pattern in intact animals.

## ACKNOWLEDGEMENTS

Our colleague Dr. K. A. French (San Diego, CA) kindly provided the juvenile leeches used for video imaging in this study. We thank A.E. Tobin for carefully reading the manuscript. We are grateful to Jim Cole of Becton and Dickinson Critical Care Systems (Ventura, CA) for the donation of the disposable pressure transducer used in this study. Supported by the NIH NS24072.

**REFERENCES**

**Boroffka I and Hamp R.** Topographie des Kreislaufsystems und Zirkulation bei *Hirudo medicinalis. Z Morph Ök Tiere* 64: 59-76, 1969.

**Calabrese RL.** The neural control of alternate heartbeat coordination states in the leech, *Hirudo medicinalis*. *J Comp Physiol* 122: 11-143, 1977.

**Calabrese RL and Feldman JL**. Intrinsic Membrane Properties and Synaptic Mechanisms in Motor Rhythm Generators. In: *Neurons, Networks, and Motor Behaviour*, edited by Stein PSG, Grillner S, Selverston AI and Stuart DG. Cambridge, Massachusetts; London, England: MIT Press, 1997, p. 119-130.

**Calabrese RL and Maranto AR.** Neural control of the hearts in the leech, *Hirudo medicinalis*. III. Regulation of myogenicity and muscle tension by heart accessory neurons. *J Comp Physiol A* 154: 393-406, 1984.

**Calabrese RL, Nadim F, and Olsen OH.** Heartbeat control in the medicinal leech: a model system for understanding the origin, coordination, and modulation of rhythmic motor patterns. *J Neurobiol* 27: 390-402, 1995.

**Calabrese RL and Peterson E.** Neural control of heartbeat in the leech, *Hirudo medicinalis*. *Symp Soc Exp Biol* 37: 195-221, 1983.

**Hammersen F, Staudte H-W, and Möhring E.** Studies of the fine structure of invertebrate blood vessels. II. The valves of the lateral sinus of the leech, *Hirudo medicinalis* L. *Cell Tiss Res* 172: 405-423, 1976.

**Hildebrandt K-P.** Circulation in the leech, *Hirudo medicinalis. J Exp Biol* 134: 235-246, 1988.

**Hill AA, Masino MA, and Calabrese RL.** Model of intersegmental coordination in the leech heartbeat neuronal network. *J Neurophysiol* 87: 1586-1602, 2002.

**Hill AAV, Masino MA, and Calabrese RL.** Intersegmental coordination of rhythmic motor patterns. *J Neurophysiol*, in press.

**Jones DR, Bushnell PG, Evans BK, and Baldwin J.** Circulation in the Giant Gippland earthworm *Megascolides australis*. *Physiol Zool* 67: 1383-1401, 1994.

**Krahl B and Zerbst-Boroffka I.** Blood pressure in the leech *Hirudo medicinalis*. *J Exp Biol* 107: 163-168, 1983.

**Kristan WB, Stent GS, and Ort CA.** Neuronal control of swimming in the medicinal leech. I. Dynamics of the swimming rhythm. *J Comp Physiol* 94: 97-119, 1974.

**Lu J, Gramoll S, Schmidt J, and Calabrese RL.** Motor pattern switching in the heartbeat pattern generator of the medicinal leech: membrane properties and lack of synaptic interaction in switch interneurons. *J Comp Physiol A* 184: 311-324, 1999.

**Maranto AR and Calabrese RL.** Neural control of the hearts in the leech, *Hirudo medicinalis.* I. Anatomy, electrical coupling, and innervation of the hearts. *J Comp Physiol A* 154: 367-380, 1984a.

**Maranto AR and Calabrese RL.** Neural control of the hearts in the leech, *Hirudo medicinalis.* II. Myogenic activity and its control by heart motor neurons. *J Comp Physiol A* 154: 381-391, 1984b.

**Pearson KG and Ramirez J-M.** Sensory Modulation of Pattern-Generating Circuits. In: *Neurons, Networks, and Motor Behaviour*, edited by Stein PSG, Grillner S, Selverston AI and Stuart DG. Cambridge, Massachusetts; London, England: MIT Press, 1997, p. 225-235.

**Thompson WJ and Stent GS.** Neuronal control of heartbeat in the medicinal leech. I. Generation of the vascular constriction rhythm by heart motor neurons. *J Comp Physiol* 111: 261-279, 1976a.

**Thompson WJ and Stent GS.** Neuronal control of heartbeat in the medicinal leech. II. Intersegmental coordination of heart motor neuron activity by heart interneurons. *J Comp Physiol* 111: 281-307, 1976b.

**Wenning A and Calabrese RL.** One Leech-Two Hearts: Matching Motor with Movement Pattern. *Soc Neurosci Abstr* 28: 465.2, 2002.

**Wenning A, Hill AAV, and Calabrese RL.** Regulation of blood pressure in the leech: Interaction of peripheral neuromodulation and central pattern. *Soc Neurosci Abstract* 26: 164:4, 2000.

**Wenning A, Hill AAV, and Calabrese RL.** Heartbeat Control in Medicinal Leeches: II. Fictive Motor Pattern. *J Neurophysiol*, submitted.

**FIGURE LEGENDS**

FIG. 1. Diagram to show diastolic filling and emptying in systole in the leech hearts and their side vessels as well as pressure profiles in a midbody segment in both coordination modes. Blood inflow is through the contractile laterodorsal and laterolateral vessels, outflow is through the lateroabdominal vessel. Directed blood flow is aided by valves and sphincters. In the peristaltic coordination mode (left), systolic pressures are around 50 mm Hg with a distinct prepulse (*). Systolic pressures are around 25 mm Hg in the synchronous coordination mode (right). Hearts are not drawn to scale.

Based on (Boroffka and Hamp 1969; Hammersen et al. 1976; Hildebrandt 1988; Krahl and Zerbst-Boroffka 1983).

FIG. 2. Diagram to show the recording of intravascular pressure with a pressure transducer from a leech heart in a minimally dissected preparation. The system is filled from a reservoir (1). The recording pipette is placed in solution close to the recording site, shut off from the reservoir, and briefly vented to outside for calibrating to atmospheric pressure (2). For pressure readings, the recording pipette and the transducer are shut off both from the reservoir and from outside (3).

FIG. 3. Consecutive images of midbody segments 8 and 10 to show the blood flow through the lateral hearts (ventral view, anterior to the left) in an intact juvenile leech. The right heart (R, bottom) is in the synchronous coordination mode,

the left heart (top, L) in the peristaltic coordination mode. Dots indicate heart sections filled with blood. Data from light intensity changes were collected from analysis windows from a corresponding area of the lateral hearts in each segment (ovals at 1190 ms) and digitized to give a numerical optical signal. The heartbeat period was 6.2 s. See also movie.

FIG. 4. Diameter changes of the heart tubes in segment 10 (top traces) correspond to changes in the optical signal captured from the same area (bottom traces): shown for both coordination modes. The largest diameter of the heart (maximal diastole, 100%) coincides with the trough of the optical signal (minimum light intensity, circle). Attainment of systole (diamond) corresponds to the start of the decrease in heart diameter. Data are from an intact juvenile leech.

FIG. 5. Intersegmental phase differences in systole in middle segments 8 to 10 on the left (L,8 to L,10; top three traces) and right (R,8 to R,10; bottom three traces) in an intact juvenile leech across a switch in coordination mode. The expanded trace on the left emphasizes the differences between the two coordination modes. The shaded box corresponds to the same heartbeat cycle as shown in Fig. 3. Diamonds indicate the systole for each heartbeat cycle connected by dotted lines for visual guidance. The solid vertical line in the expanded optical signals (left) indicates the time that the first heart segment attains systole (segment 10 on the peristaltic side, segment 8 on the synchronous side). Switching occurred during the third cycle and was reciprocal. The average phase difference is indicated for each

segment and is referenced to ipsilateral heart segment 10 (0% phase; boxed diamonds).

FIG. 6. Examples of the intersegmental phase differences in systole (diamonds) for front segments 3 to 6 (left) and rear segments 12 to 18 (right) from two intact juvenile leeches. In the front segments, systole progresses rear-to-front on the peristaltic side and occurs almost simultaneously on the synchronous side (left), while the rear segments constrict nearly simultaneously in both coordination modes (right). Note that systole is brief in front segments 3 and 4. Mean phase differences are referenced to segment 6 (front) and to segment 16 (rear).

FIG. 7. *A*: Phase does not vary with heartbeat period in intact juvenile (triangles) or adult (diamonds) leeches. The phase difference between systole in segments 11 (phase marker) and 8 is shown for the peristaltic (red) and synchronous (blue) coordination mode with respect to the heartbeat period. *B*: Phase diagram to show diastole (small symbols) and systole (large symbols) of heart segments 3 to 18 on one body side in the peristaltic (red) and synchronous (blue) coordination mode for intact juvenile (left; diamonds) and adult (right; circles) leeches. The phase marker is systole in segment 10 (0% phase; vertical dotted line). Average (± SD) of average measurements from 3 to 15 heartbeats per segment from 8 (juvenile) and 9 (adult) preparations.

FIG. 8. Side-to-side coordination of systole in juvenile (left) and adult (right) leeches. The heart in segment 10 on the peristaltic side is the reference segment, and its systole is the phase marker (0% phase; vertical dotted line). The synchronous side is shifted by 60.2% for juvenile and 62.1% for adult leeches. The peristaltic side has been duplicated and shifted by 100% (vertical dotted line) to illustrate intersegmental phase differences in the rear. Data are from Figure 7.

FIG. 9. Diameter changes of a left heart in segment 14 (top trace) in relation to the corresponding heart motor neuron activity (bottom trace (Y(L,14)) across a switch from the synchronous to the peristaltic coordination mode. The upper horizontal dashed line indicates the average end-diastolic diameter for this preparation (= 100%). A star below each burst indicates the median spike. Vertical dotted lines help to visualize the timing of systole (short horizontal dashed lines) with respect to the median spike of each heart motor neuron burst. The intraburst frequency is represented by a solid line (center). Coordination modes were assessed by simultaneously recording from a heart motor neuron in a different segment (trace not shown). The cartoon (bottom) shows the arrangement for simultaneous imaging the heart and *en passant* recording of heart motor neuron activity.

FIG. 10. Phase difference between heart constriction (assessed as changes in the heart diameter (circles)) and the corresponding heart motor neuron burst, illustrated by its spike frequency envelope (solid green line) is shown for segments 4, 7, 10, and 14 (N = number of preparations) in the peristaltic (red) and synchronous

(blue) coordination mode. For the heart diameter, 100% corresponds to diastole (upper dashed line, shown for segment 4 only). Systole (lower dashed line, blue) was defined as a constriction to 20% of the maximum constriction of the heart segment. The range of the timing of systole with respect to the heart motor neuron burst across preparations is indicated for each segment by the blue horizontal bar. Heart diameters were measured in 2 – 4 heartbeat cycles per coordination mode. Average (± SD) of average measurements. Intraburst spike frequencies and heart diameters were binned in 4% phase intervals.

FIG. 11. Extracellular recordings from the cell body of a heart accessory neuron (HA) and the heart nerves on the contralateral side (see Fig. 1*A* of Wenning et al. (2003) for a description of the heart innervation) in different segments along the body axis. *A*: Cartoon of experimental setup. *B*: An action potential recorded in the cell body of the right heart modulatory neuron in segment 6 (HA(R,6)) gives rise to a small spike (*) with a fixed delay in the left anterior vascular nerves of segments 9 (AVN(L,9) and 12 (AVN(L,12) (*B*: 8 superimposed traces). *C*: An action potential in the cell body of the right heart modulatory neuron in segment 5 HA(R,5) gives rise to a small spike (*) in the left anterior vascular nerve of segment 3 (15 superimposed traces). *D*: Extracellular recordings from the Y nerves in segments 5 and 10 on the left side (top and middle trace) and the cell body of the heart accessory neuron in segment 6 on the right side (HA(R,6)). Bursting is irregular in the heart modulatory neuron of segment 5 (top trace, *; activity was verified by simultaneous recordings from the HA(R,5) cell body; trace not shown). Spikes are grouped into

well-defined bursts in the heart modulatory neuron of segment 6 (bottom trace). The phase difference between the bursts of action potentials recorded in heart motor neurons in segment 5 (Y(L,5); top trace) and 10 (Y(L,10); center trace) defined the coordination mode.

FIG. 12. Intravascular pressure recordings in a semi-intact preparation from the heart in segment 8 on the right body side (Heart(R,8)) while simultaneously recording intracellularly from the heart modulatory neuron in segment 6 on the contralateral side (HA(L,6)) (cartoon, right). *A*: High systolic pressures are found in the peristaltic coordination mode and low systolic pressures in the synchronous coordination mode. *B*: Depolarization of the heart modulatory neuron causes an increase in systolic and diastolic blood pressure in the synchronous coordination mode. *C*: Hyperpolarization of the heart modulatory neuron causes a decrease in the systolic pressure in both coordination modes. The asterisks denote the switches between coordination modes.

Table 1. *Switch period and number of beats between switches in juvenile intact leeches*

| *Number of switch cycles per preparation* | *Switch period (s)* | *Coefficient of variation* | *Number of beats per switch period rounded to the nearest integer* | *Coefficient of variation* |
|---|---|---|---|---|
| 10 | 113±13 | 0.12 | 18±2 | 0.11 |
| 7 | 86±8 | 0.09 | 20±2 | 0.10 |
| 8 | 43±7 | 0.16 | 13±2 | 0.15 |
| 7 | 84±11 | 0.13 | 18±3 | 0.17 |
| 12 | 96±10 | 0.10 | 20±2 | 0.10 |

Values are means±SD.

Figure 1
Wenning, Cymbalyuk, and Calabrese

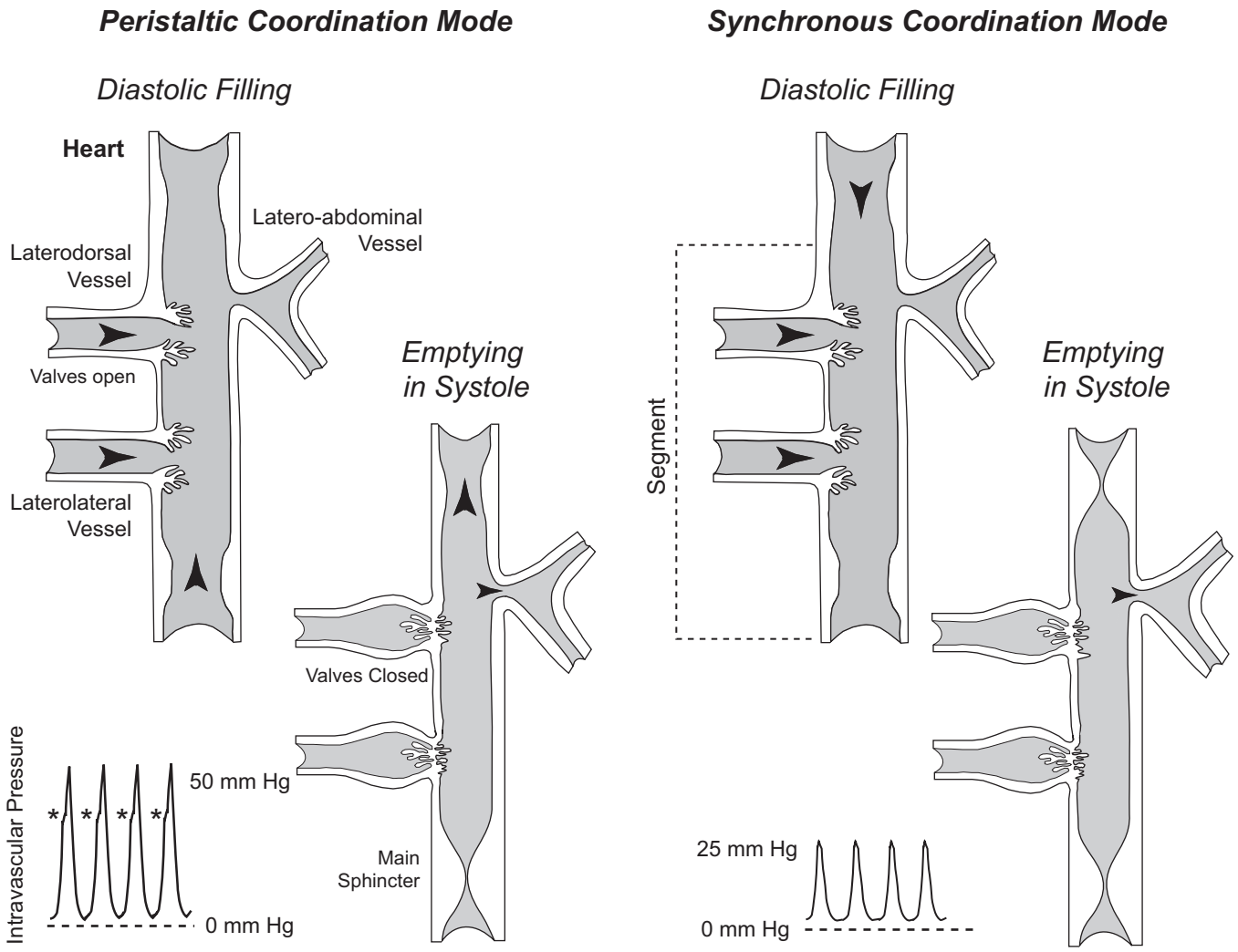

Figure 2
Wenning, Cymbalyuk, and Calabrese

Intravascular Pressure Recording from the Heart

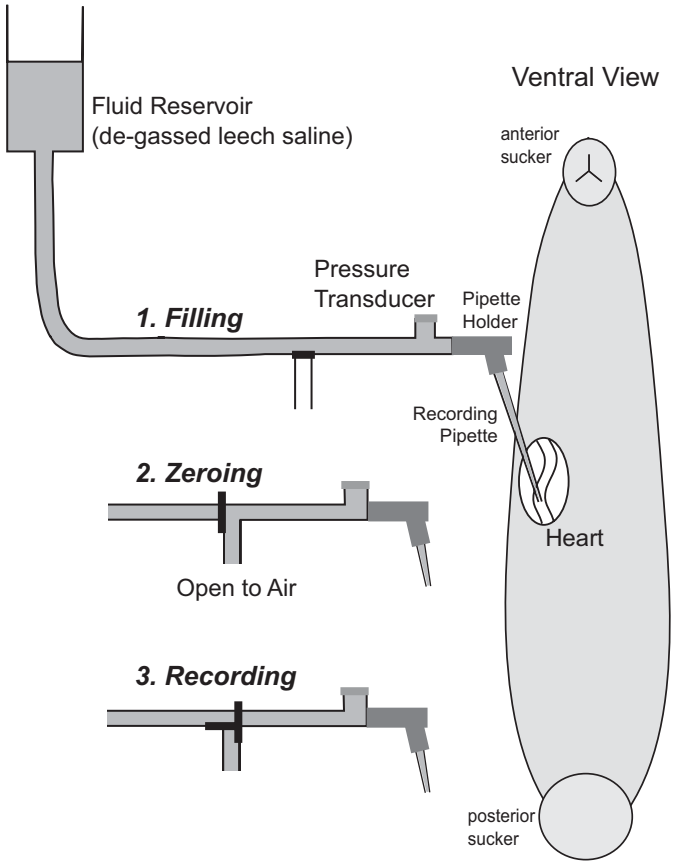

Figure 3
Wenning, Cymbalyuk, and Calabrese

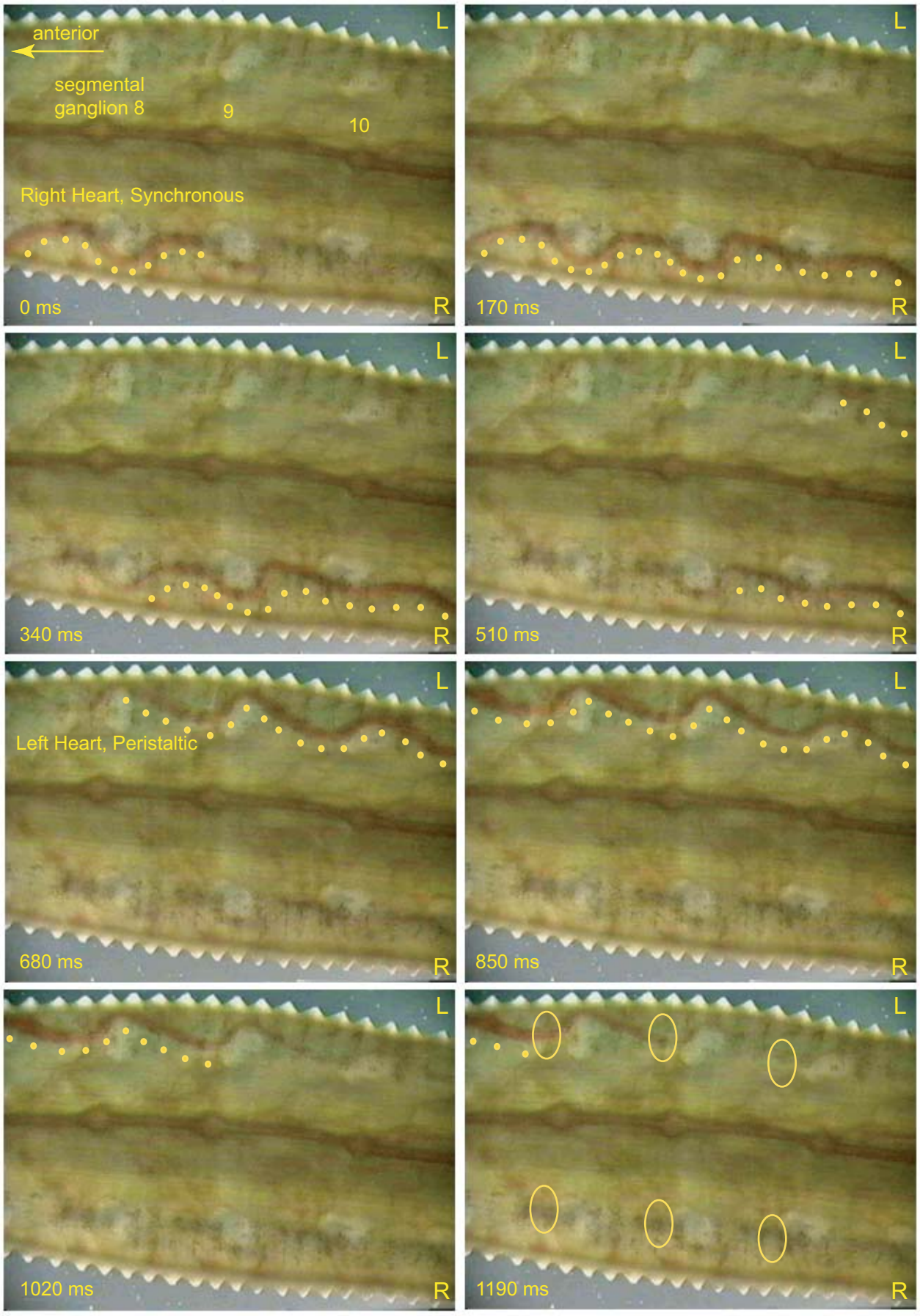

Figure 4
Wenning, Cymbalyuk, and Calabrese

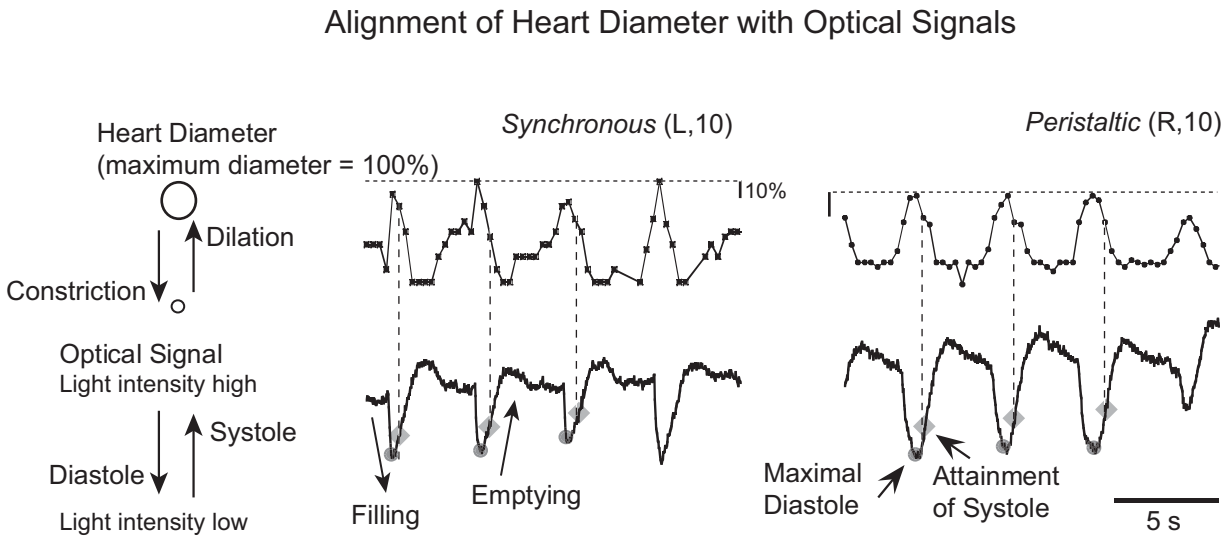

Figure 5
Wenning, Cymbalyuk, and Calabrese

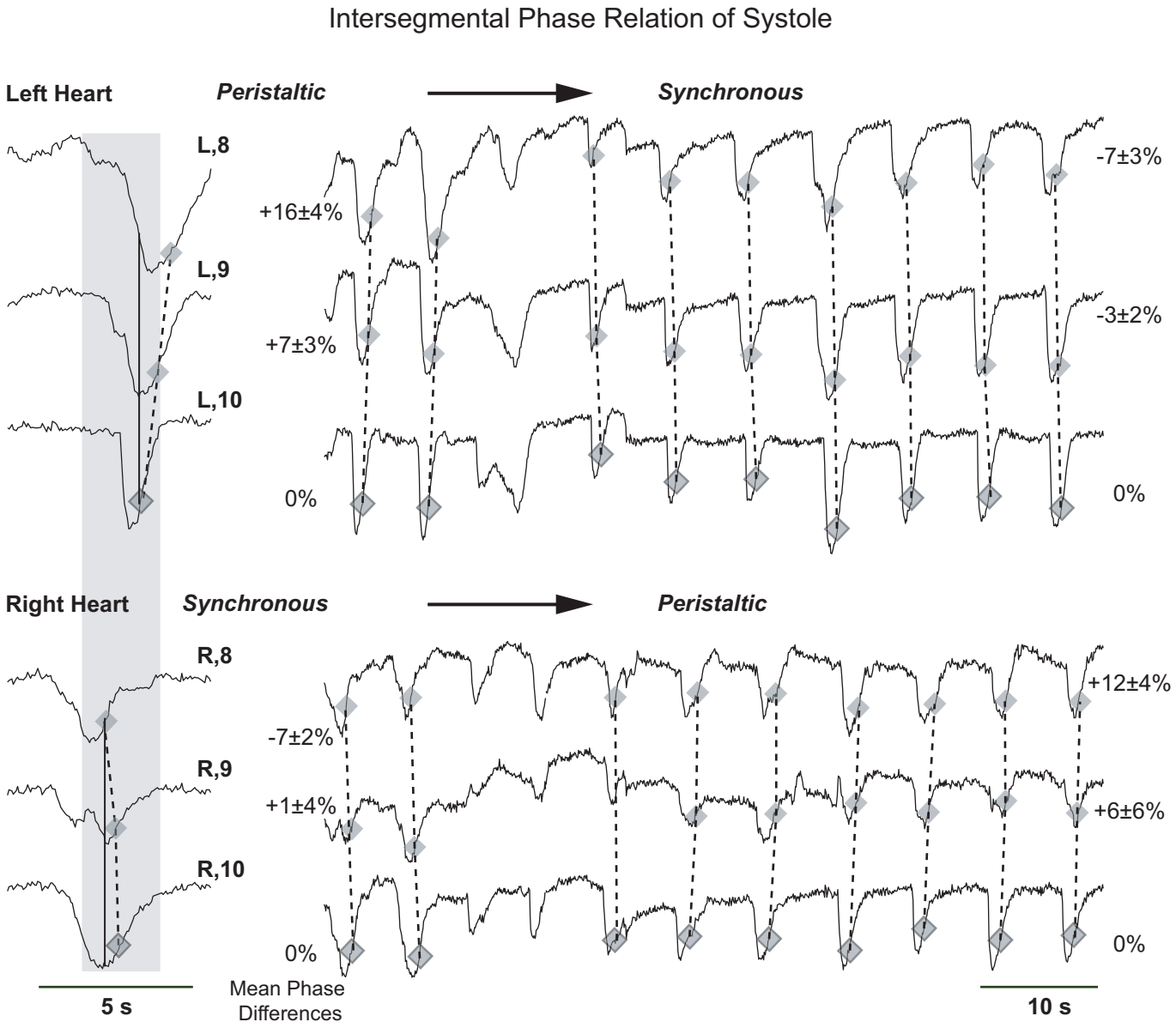

Figure 6
Wenning, Cymbalyuk, and Calabrese

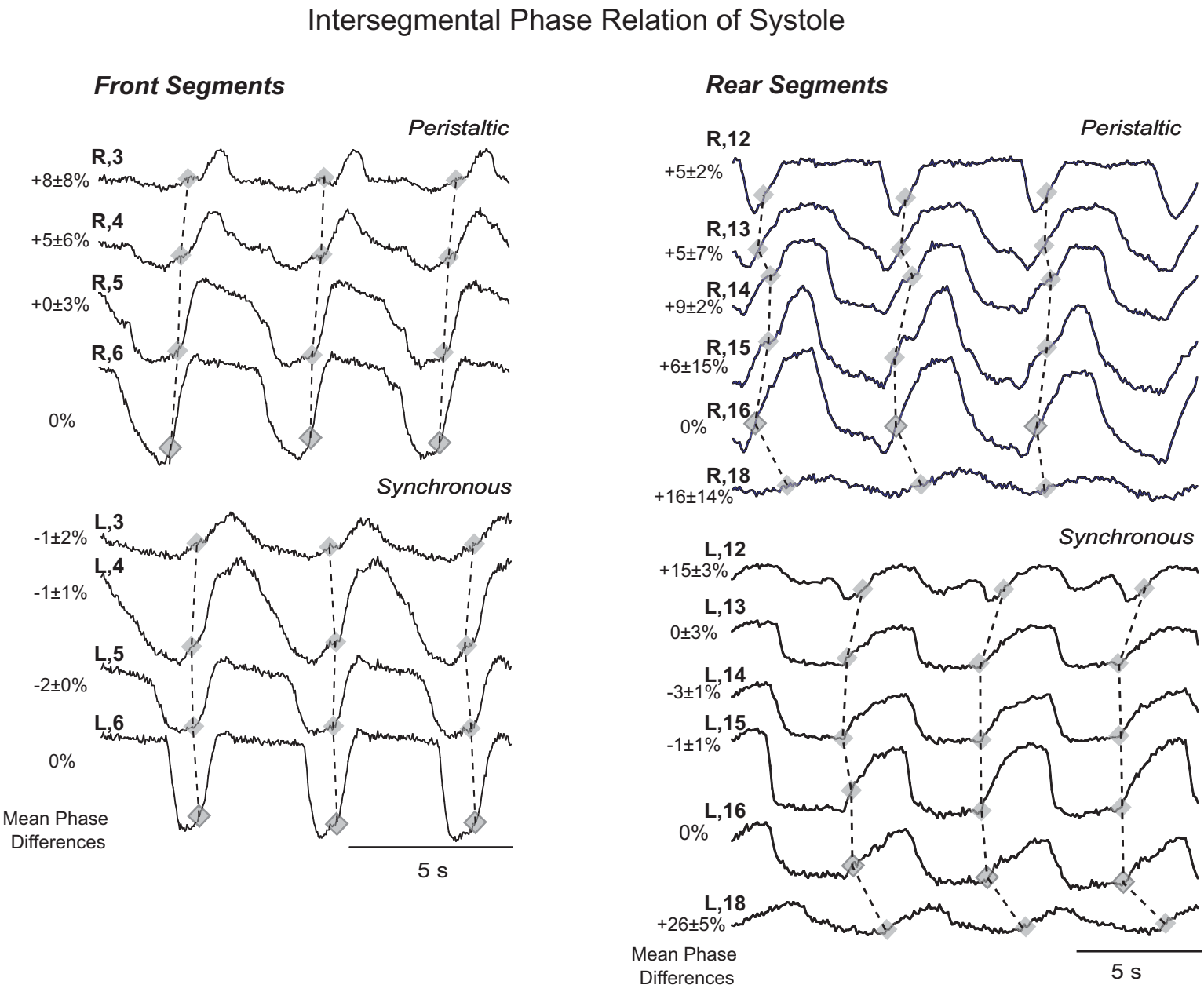

# Figure 7

Wenning, Cymbalyuk, and Calabrese

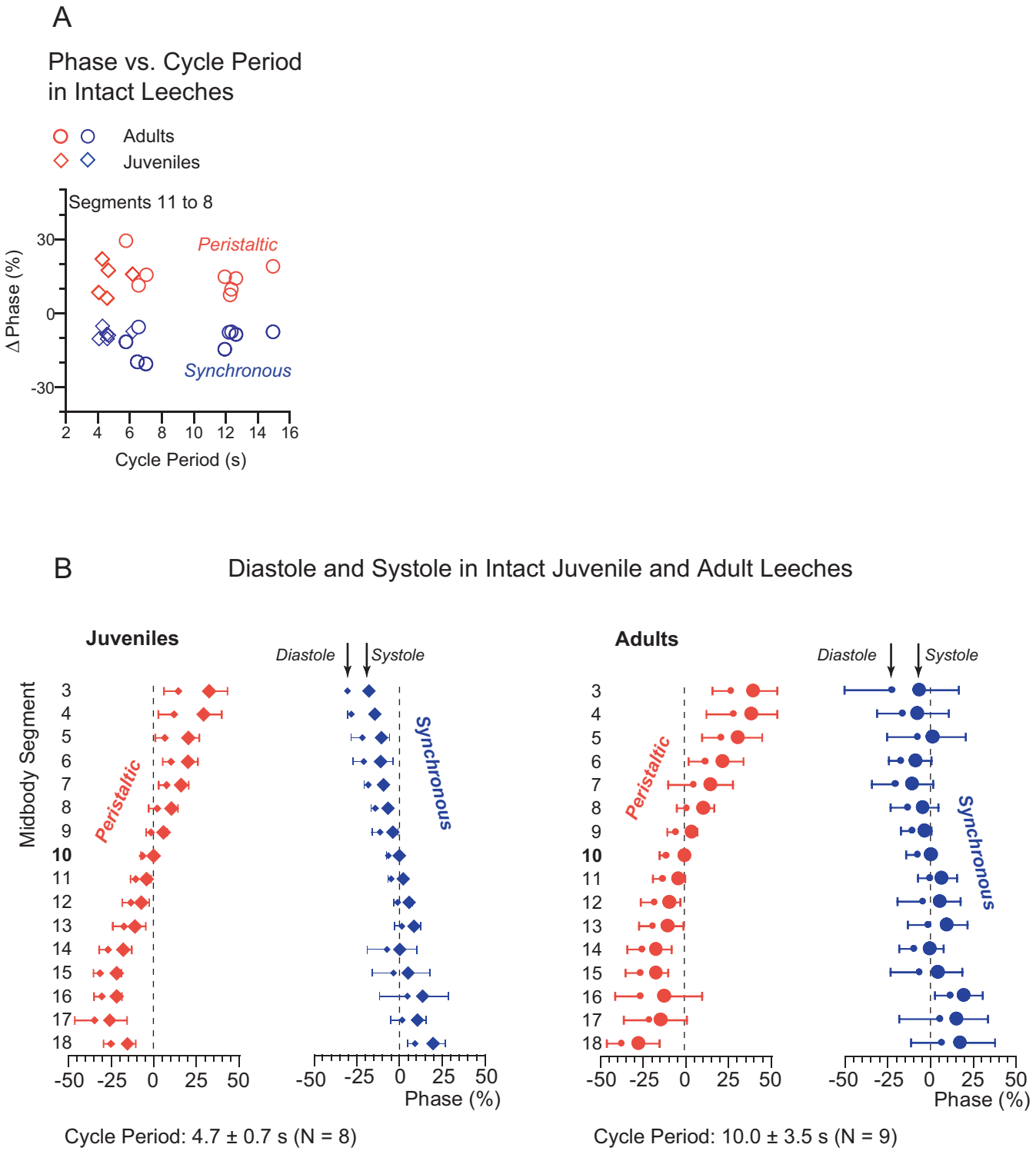

Figure 8
Wenning, Cymbalyuk, and Calabrese

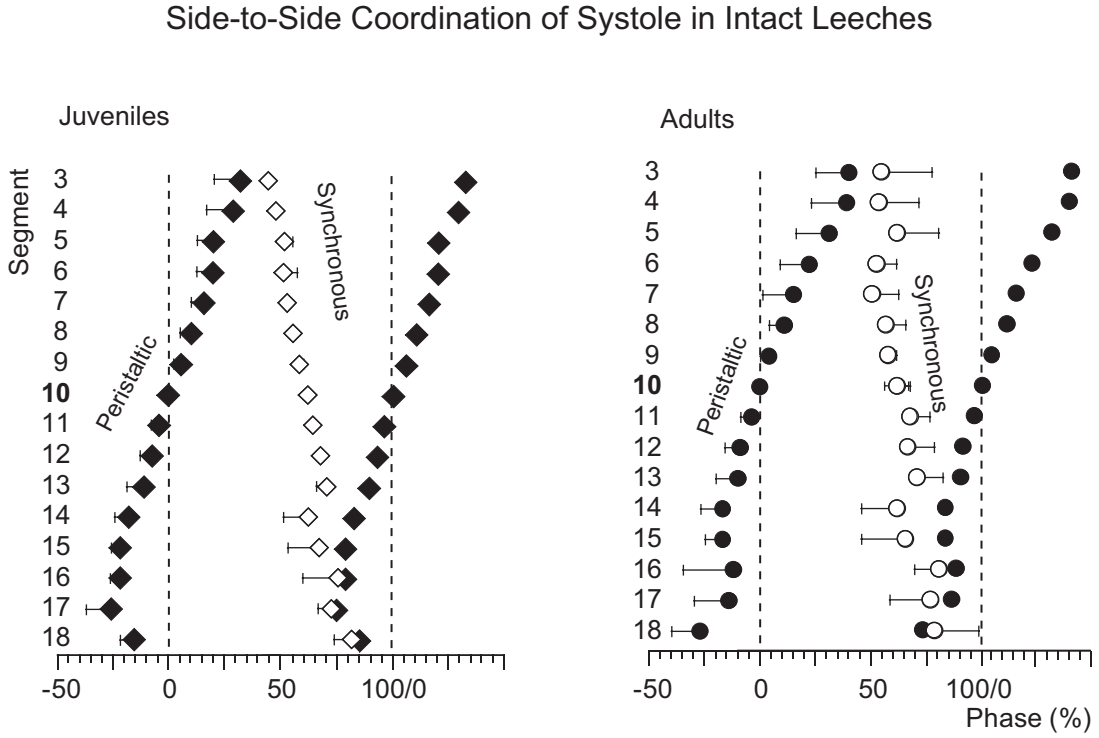

Figure 9
Wenning, Cymbalyuk, and Calabrese

Relation of Heart Constriction and Heart Motor Neuron Activity across a Switch

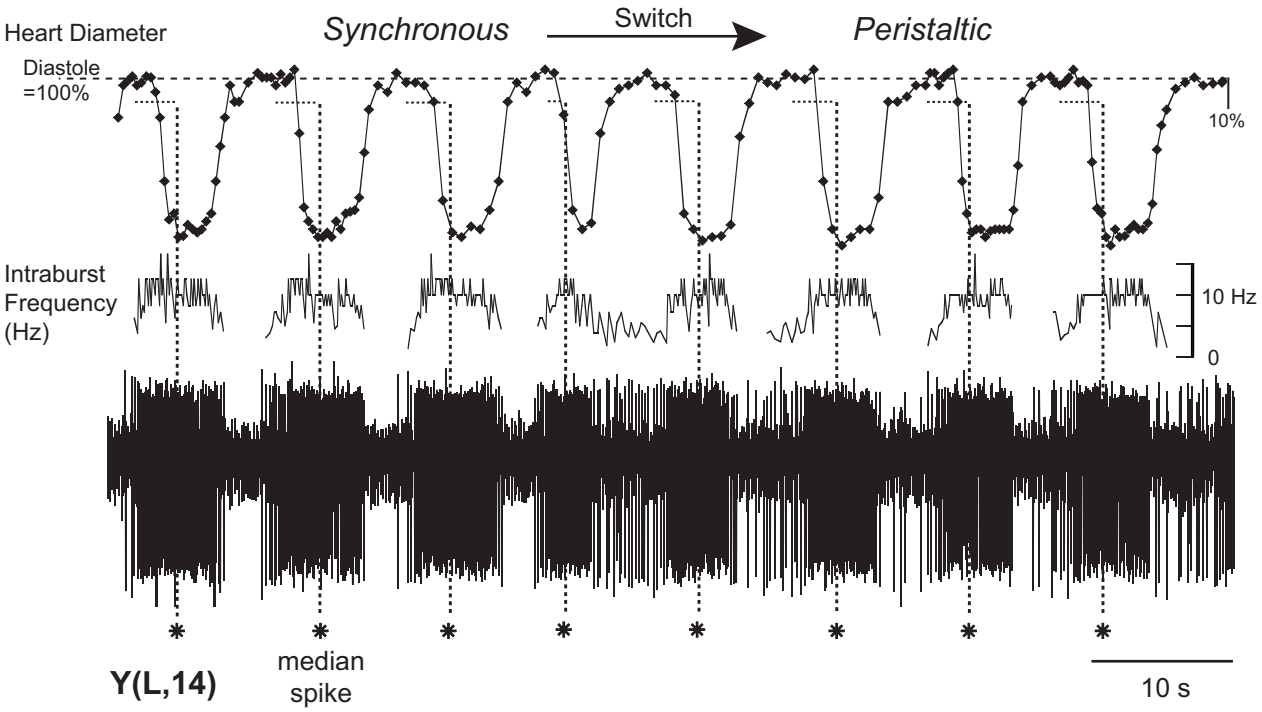


Recording of Heart Constrictions and Heart Motor Neuron Activity

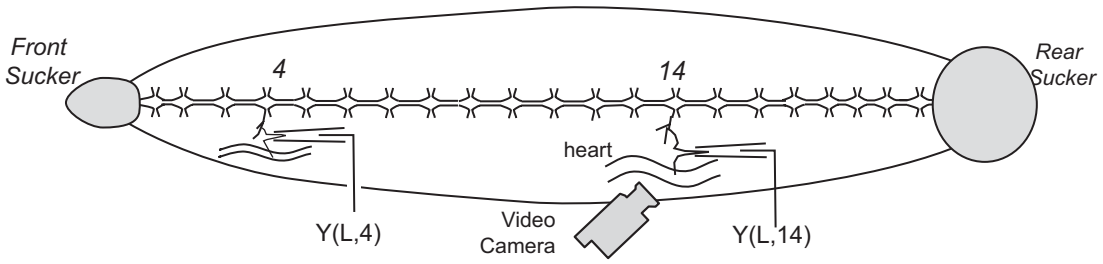

Figure 10
Wenning, Cymbalyuk, and Calabrese

Phase Relation of the Heart Motor Neuron Activity and Heart Constriction

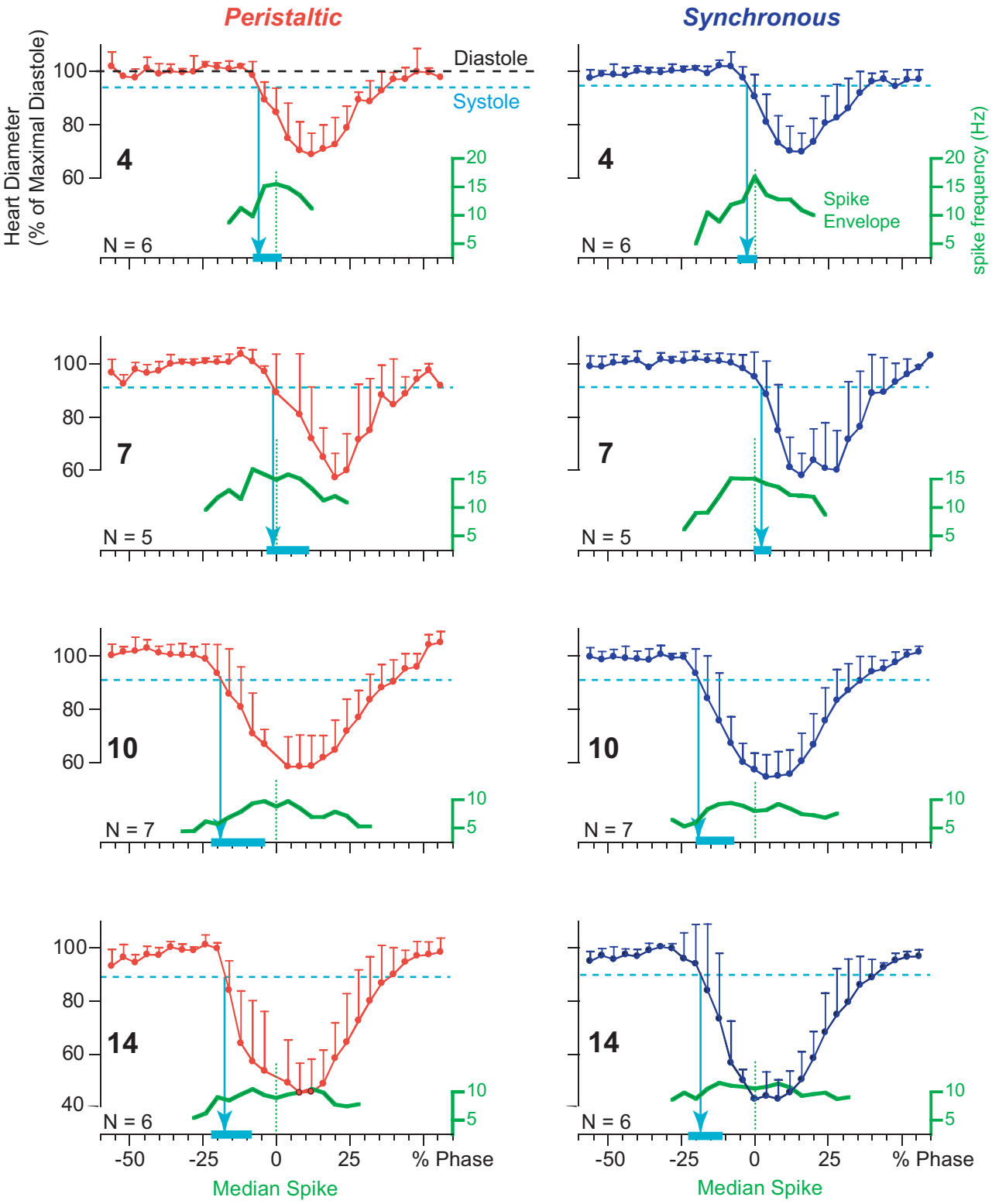

Figure 11
Wenning, Cymbalyuk, and Calabrese

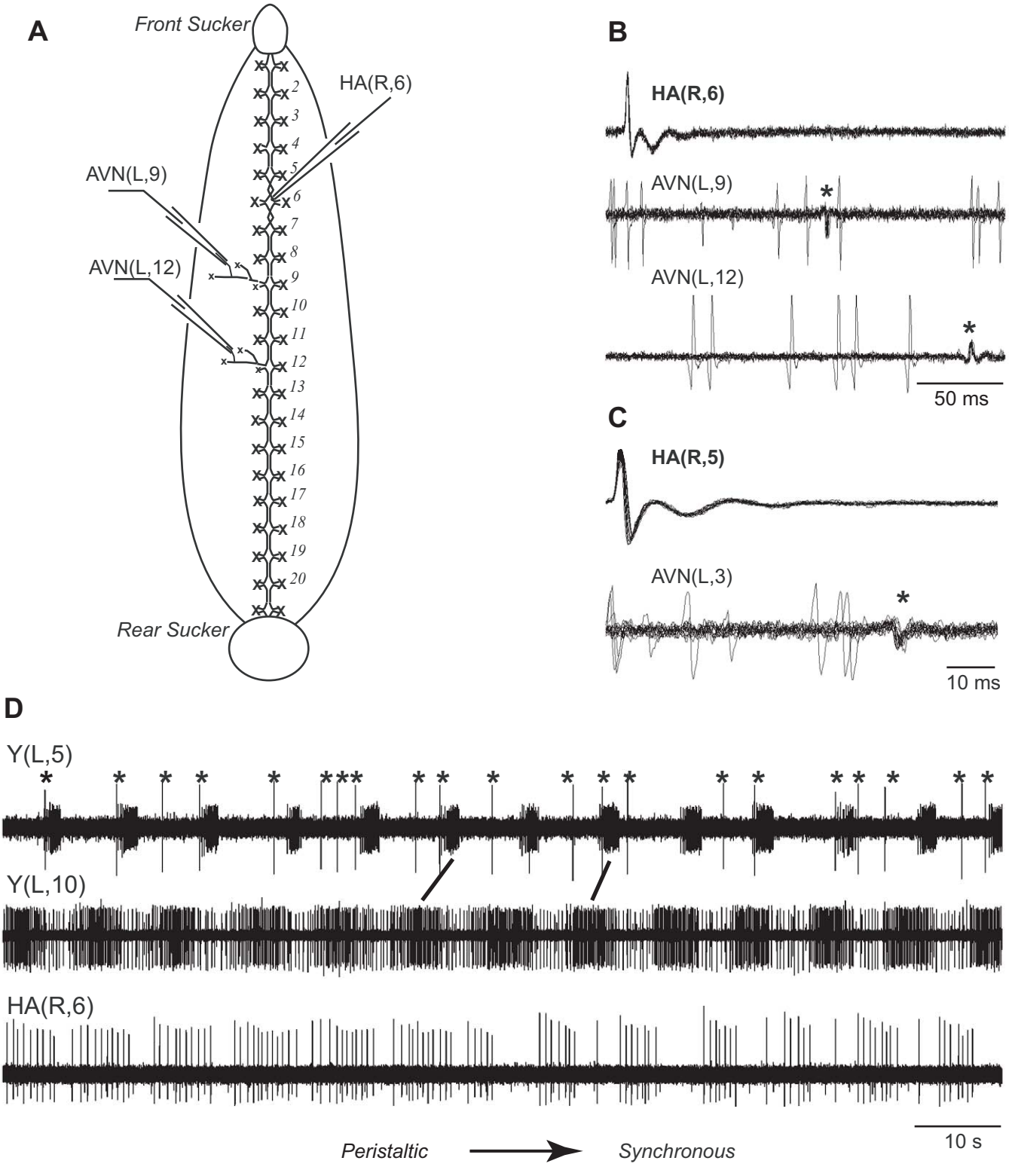

# Figure 12

Wenning, Cymbalyuk, and Calabrese